PHYSICAL REVIEW B, VOLUME 63, 121307(R)

Dynamic band-structure modulation of quantum wells by surface acoustic waves

T. Sogawa,[1,2] P. V. Santos,[1,*] S. K. Zhang,[1] S. Eshlaghi,[3] A. D. Wieck,[3] and K. H. Ploog[1]
[1]*Paul-Drude-Institut für Festkörperelektronik, Hausvogteiplatz 5-7, 10117 Berlin, Germany*
[2]*NTT Basic Research Laboratories, 3-1, Morinosato-Wakamiya, Atsugi, Kanagawa 243-0198, Japan*
[3]*Lehrstuhl für Angewandte Festkörperphysik, Ruhr-Universität Bochum, 44780 Bochum, Germany*
(Received 13 November 2000; published 7 March 2001)

The dynamical modulation of the band structure of GaAs quantum wells by a surface acoustic wave (SAW) is investigated using photoluminescence (PL) spectroscopy. The strain field of the SAW modulates the excitonic transitions, leading to a splitting and to a polarization anisotropy of the excitonic PL lines. The oscillator strength of the split line gives direct information about the spatial distribution of carriers in the potential modulation induced by the SAW.

DOI: 10.1103/PhysRevB.63.121307 PACS number(s): 77.65.Dq, 77.65.Ly, 78.55.Cr

Quantum confinement of carriers in artificial semiconductor structures has contributed to fundamental scientific studies as well as to the development of electrical and optical devices.[1] In particular, basic physical properties such as the electronic band gap and the strength of excitonic transitions can be controlled in quantum-well (QW) structures by sophisticated epitaxial growth techniques based on the static control of material composition and dimensions. Various approaches have been demonstrated to further reduce the dimensionality of the structures to one or zero dimensions. The dimensionality reduction, however, has normally been accompanied by deleterious effects induced by lateral interfaces and/or by fluctuations in structural dimensions.

Surface acoustic waves (SAW's) provide an alternative way of introducing a dynamic one- or two-dimensional lateral modulation of the band structures of QW structures. Although the presently achieved modulation periods (equal to the SAW wavelength λ_{SAW}, normally between 1 and 10 μm) are much larger than typical QW thicknesses, the modulation is perfectly periodic and the material is not subject to the deleterious effects introduced by interfaces and by doping impurities. As a consequence, the carriers are expected to retain a high mobility.

Band modulation introduced by SAW's differs qualitatively from that induced by a static modulation, because its time and spatial dependence allows for dynamic control of material properties. As a consequence, the carrier dynamics in SAW fields also depends on the transport properties, which define how the carriers follow and how they screen the modulation. The interplay between the SAW acoustic and piezoelectric fields with the transport properties makes it difficult to identify the mechanisms for the interaction between the SAW and photogenerated carriers. In this communication, we employ photoluminescence (PL) spectroscopy to elucidate the mechanism for the modulation of the band structure of GaAs QW's by a SAW. We demonstrate that the spatial modulation of the band edges for low SAW intensities is primarily due to the SAW strain field. The latter splits the PL line into a doublet with different polarization properties. The relative intensities of the doublet components, in contrast, are mainly determined by the piezoelectric field of the SAW, and directly reflect the microscopic distribution of photogenerated carriers in the modulated potential.

The investigations were performed on a sample containing several GaAs single QW's with short period (AlAs/GaAs) superlattice barriers grown on (001) GaAs by molecular beam-epitaxy.[2] We will report results obtained on three QW's (QW_1–QW_3, with thicknesses of 19.8, 15.4, and 12.2 nm, respectively) located between 300 and 400 nm below the surface. Rayleigh SAW's propagating along the $x'=[110]$ surface direction were generated by split-finger interdigital transducers [cf. inset of Fig. 1(a)], designed for operation at a wavelength $\lambda_{SAW}=5.6\,\mu$m [corresponding to a frequency $\omega_{SAW}/(2\pi)=520$ MHz at 16 K]. The PL experiments were performed with the sample mounted in an optical cryostat ($T=16$ K) using a confocal microscope with coincident illumination and detection areas with a diameter ρ_0 of about 2 μm. The cw radiation from a Ti-sapphire laser ($\lambda_L=750$ nm) was used for PL excitation. The SAW intensity will be expressed in terms of the nominal radio-frequency (rf) power P_{rf} (in dBm) applied to the transducer. rf coupling losses and attenuation of the SAW fields by carriers make the actual SAW acoustic power lower than P_{rf} by $\Delta P=12-18$ dB, as determined from rf transmission measurements.

Figure 1(a) displays PL spectra of QW_1–QW_3 recorded on the propagation path of the SAW for different rf powers levels. In the absence of rf excitation, each QW displays a sharp line (linewidths <0.6 meV) with an energy $E_{e\text{-hh}}$ corresponding to the electron heavy-hole (e-hh) transition. The weaker lines indicated by dashed arrows with energies of 1.5328 and 1.5437 eV are associated with the electron–light-hole (e-lh) transitions of QW_1 and QW_2, respectively (the e-lh line for QW_3 is not shown). Under the influence of a SAW, the PL intensity becomes strongly suppressed (note the logarithmic vertical scale). The suppression is attributed to (i) the ionization of the excitons, and (ii) the sweep of the electron-hole pairs out of the μ-PL detection spot by the longitudinal componente $F_{x'}$ of the piezoelectric field accompanying the SAW.[3–5]

A remarkable feature in Fig. 1(a) is the splitting of the PL lines into two components with energies $E^{+,-}_{e\text{-hh}}=E^{0}_{e\text{-hh}}+\Delta E^{+,-}_{e\text{-hh}}$ ($E^{+,-}_{e\text{-lh}}=E^{0}_{e\text{-lh}}+\Delta E^{+,-}_{e\text{-lh}}$ for the e-lh transitions) with increasing SAW amplitude. This splitting has not been observed in previous experiments:[3–5] it becomes apparent here due to the very narrow PL linewidths.

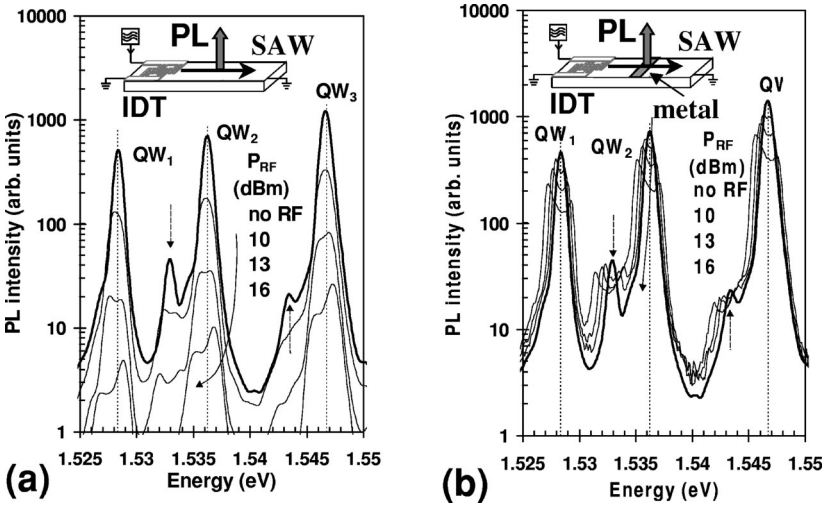

FIG. 1. Photoluminescence spectra of QW_1–QW_3 recorded at 16 K (a) on the free sample surface, and (b) over the semitransparent metal stripe (cf. inset), for different rf power levels applied to the SAW transducer. The dashed arrows indicate the e-lh transitions for QW_1 and QW_2 in the absence of rf excitation (thick curves).

A Rayleigh SAW possesses, in addition to the strain field, a piezoelectric field with longitudinal ($F_{x'}\|x'$) and transverse ($F_z\|z$) components. In order to determine their contribution to the splittings, PL spectra were also recorded on a stripe of semitransparent nickel-chromium film deposited on the SAW propagation path, as is illustrated in the inset of Fig. 1(b). Since the QW's are located close to the surface, the thin metal film effectively short circuits the longitudinal component $F_{x'}$ and also modifies F_z.[4] The SAW strain field, however, remains practically undisturbed by the metal. The integrated intensity of the PL lines measured under these conditions [Fig. 1(b)] shows no appreciable suppression under a SAW. The splitting, however, remains approximately the same as in Fig. 1(a), thus indicating that it is not associated with the SAW piezoelectric field.

We attribute the PL splitting to the dynamic modulation of the electronic transition energies induced by the strain accompanying the SAW. In order to demonstrate this point, we calculated the energy shifts of the electron (ΔE_e), heavy-hole ($\Delta E_{\rm hh}$), and light-hole ($\Delta E_{\rm lh}$) bands induced by the strain. The calculations proceeded in two steps. First, the displacement field of the Rayleigh wave with components $u_{x'}(x',z)$ and $u_z(x',z)$ along the $x'=[110]$ and $z=[001]$ directions, respectively, were determined following the procedure described in Ref. 6 by neglecting the differences between the acoustic properties of GaAs and AlAs. In the second step, the strain field obtained from the previous calculations was used to determine the energy shifts of the electronic states. The modulation of the lowest conduction band was determined from the hydrostatic component of the strain field using a band deformation potential $a=-8.6\,\text{eV}$.[7] In order to determine the modulation of the upper valence bands, we solved the Pikus-Bir effective strain Hamiltonian[8] $\mathcal{H}_{\rm PB}$ within the multiplet $|J=\frac{3}{2},\ m_j=\pm\frac{3}{2},\pm\frac{1}{2}\rangle$ by simultaneously including the hh-lh energy splitting induced by the QW confinement. Band deformation potentials $a=0.4\,\text{eV}$, $b=-2.0\,\text{eV}$, and $d=-5.4\,\text{eV}$ were used for the valence band.[7] For the small strains induced by the SAWs (of the order of 10^{-4}), the shifts of the band edges were found to be approximately the same for all QW's.

Figure 2(a) displays spatial profiles of the strain-induced shifts of the band edges plotted as a function of the phase $\phi=k_{\rm SAW}x'-\omega_{\rm SAW}t$, where $k_{\rm SAW}\equiv 2\pi/\lambda_{\rm SAW}$. The calculations were performed for QW_3 for a SAW with a linear power density $P_l=8.3\,\text{W/m}$, where P_l denotes the ratio between the acoustic power and the width w of the SAW beam. The larger e-hh and e-lh transition energies at $\phi=\pi/4$ coincide with the position of maximum convex surface curva-

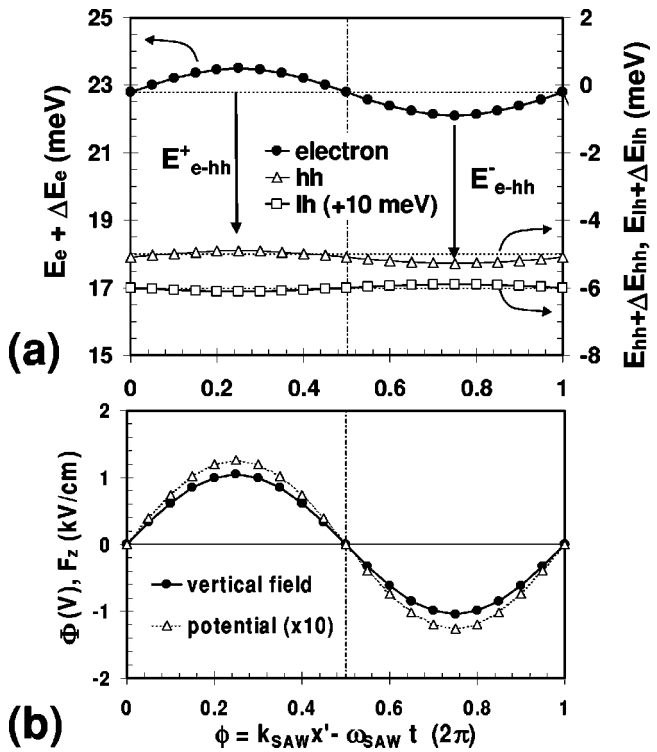

FIG. 2. (a) Strain-induced modulation ΔE_i of the electron ($i=e$), heavy hole ($i=$hh), and light hole ($i=e$) energy levels of QW_3, and (b) the piezoelectric potential Φ (triangles) and vertical component of the piezoelectric field F_z (dots) induced by a SAW with $P_l=8.3\,\text{W/m}$ as a function of the phase angle ϕ. The shifts in (a) are added to the corresponding confinement energies E_i relative to the band edges of bulk GaAs.

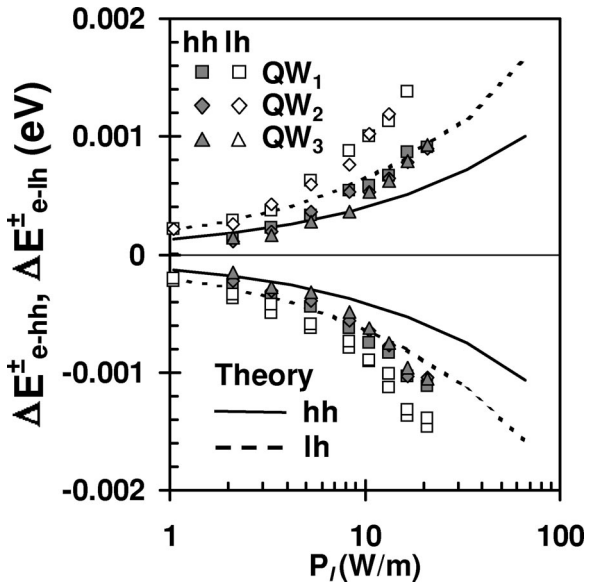

FIG. 3. Energy shifts $E^{\pm}_{e\text{-hh}}$ and $E^{\pm}_{e\text{-lh}}$ of the heavy- and light-hole transitions, respectively, for QW_1-QW_3 as a function of the rf power applied to the transducer (symbols). The solid and dashed lines display the calculated splittings of the heavy and light-hole levels.

ture and maximum compressive hydrostatic strain.

During a cw PL measurement, the energy of the e-hh transition vary approximately sinusodially under the detection spot (with diameter $<\lambda_{\mathrm{SAW}}$) around the average value $E^0_{e\text{-hh}}$ according to $E_{e\text{-hh}}=E^0_{e\text{-hh}}+\Delta E^0_{e\text{-hh}}\sin(\omega_{\mathrm{SAW}}t)$. Here $\Delta E^0_{e\text{-hh}}=\Delta E^+_{e\text{-hh}}\sim|\Delta E^-_{e\text{-hh}}|$ denotes the amplitude of the band-gap modulation. For PL excitation energies far above the fundamental gap, the carrier generation rate will not be substantially affected by the modulation. If their mobility is low (this restriction will be lifted later), the carriers will recombine close to the generation region. In this case, the energy dependence of the time-averaged PL intensity $I_{\mathrm{PL}}(E)$ becomes

$$I_{\mathrm{PL}}(E)\sim 1/\sqrt{1-\chi^2},\quad \chi\equiv[(E-E^0_{e\text{-hh}})/\Delta E^0_{e\text{-hh}}] \qquad (1)$$

for $|\chi|<1$. The discontinuities of $I_{\mathrm{PL}}(E)$ at the energies $E^0_{e\text{-hh}}\pm\Delta E^0_{e\text{-hh}}$ (which disappear when a finite PL linewidth is taken into account) lead to the peaks in the PL spectrum. Similar considerations apply to the e-lh transitions.

Figure 3 compares the strain-induced shifts $\Delta E^{\pm}_{e\text{-hh}}$ and $\Delta E^{\pm}_{e\text{-lh}}$ for SAW's with different powers P_l (symbols) with the predictions of the model described above (lines). For the experimental data, P_l was determined from the nominal rf power P_{rf} by assuming an effective coupling loss $\Delta P=12$ dBm. The dependence of the PL splitting on the SAW amplitude is well reproduced by the calculations, although the absolute magnitudes are underestimated (the discrepancies become even larger for higher ΔP). The uncertainties in the determination of the amplitude of the SAW fields, however, hinders a precise comparison between experimental and calculated values.

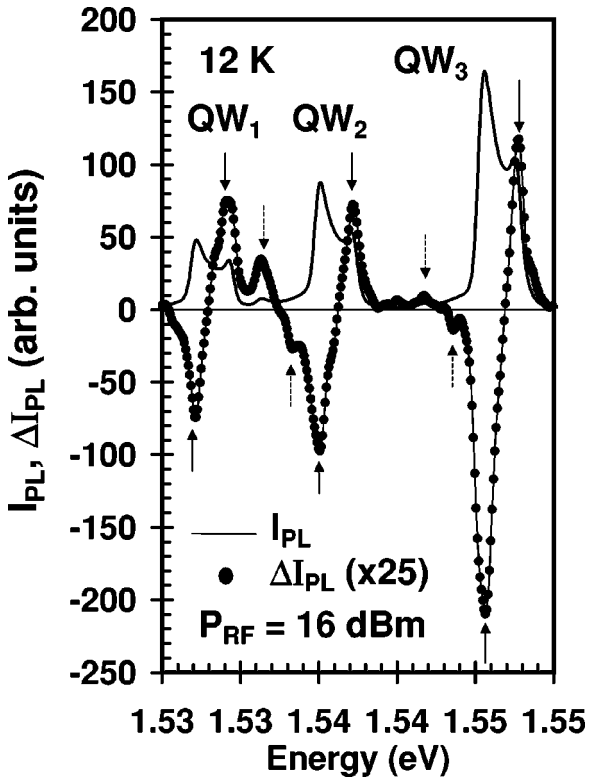

FIG. 4. Average photoluminescence (I_{PL}) and its polarization anisotropy ($\Delta I_{\mathrm{PL}}=I_{\mathrm{PL}x'}-I_{\mathrm{PL},y'}$) measured under a metal stripe for $P_{\mathrm{rf}}=16$ dBm. The solid (dashed) arrows mark the e-hh (e-lh) doublets.

The polarization of the PL gives additional evidence for the role of the strain in the splitting of the PL lines. The SAW strain reduces the tetragonal symmetry of the QW's and leads to different optical responses for polarizations parallel (x') and perpendicular ($y'\|[1\bar{1}0]$) to the SAW propagation direction.[9] Polarization-dependent matrix elements M for dipole-allowed optical transitions can be directly calculated from the wave functions obtained from the diagonalization of the strain Hamiltonian $\mathcal{H}_{\mathrm{PB}}$. The calculated relative polarization anisotropy $\delta I_{\mathrm{PL}}=2(M^2_{x'}-M^2_{y'})/(M^2_{x'}+M^2_{y'})$ can be expressed as $\delta I_{\mathrm{PL}}=\delta I^0_{\mathrm{PL}}\sin\phi$. For QW_3, $\delta I^0_{\mathrm{PL}}=0.062(-0.19)$ for the e-hh(e-lh) transition. Negative and positive anisotropies are expected for the lower- and higher-energy doublet components of the e-hh line, respectively. An opposite behavior is expected for the e-lh transitions.

The solid and dotted lines in Fig. 4 reproduce the average photoluminescence $(I_{\mathrm{PL},x'}+I_{\mathrm{PL},y'})/2$ and the difference $\Delta I_{\mathrm{PL}}=I_{\mathrm{PL},x'}-I_{\mathrm{PL},y'}$ between the PL emission with polarizations along $x'(I_{\mathrm{PL},x'})$ and $y'(I_{\mathrm{PL},y'})$, respectively.[10] For each QW, the signs of the e-hh and e-lh (arrows) anisotropy exactly follow the predictions of the previous paragraph. Also, the maximum anisotropy for the e-hh lines of QW_3, of approximately 5.5%, compares well with the value of 6.2% from Fig. 2(b).

Until now, we have disregarded the dynamics of photogenerated carriers in the spatially modulated SAW potential. In this case, equal oscillator strengths are expected for the two components of the PL doublet [cf. Eq. (1)]. In the following,

we demonstrate that the dynamic carrier redistribution in the SAW potential leads to a transfer of oscillator strength between the two doublet components. For static modulations, the hh (p) and the electron (n) densities are expected to peak at the minimum and maximum of the potential profile, respectively. For the dynamic modulation by a SAW, however, the carriers only follow the moving potential if their mobilities μ exceed $v_{\mathrm{SAW}}/F_{\mathrm{eff}}$ where v_{SAW} denotes the SAW propagation velocity and $F_{\mathrm{eff}}=|\partial\Delta E_i/\partial x'|_{\max}$ the effective field created by the modulated energy-band profile E_i. For low F_{eff}, this conditions may be satisfied for the highly mobile electrons ($\mu_e>\mu_h$), but not for holes. Therefore, even though the ambipolar diffusion dictates the same average velocity v_{SAW} for both electrons and holes, the latter will have, for every time t, a much wider spatial distribution in the SAW field as the electrons. The spatial distribution of the recombination probability, proportional to np, will then reflect that of the electronic distribution n.

If the longitudinal piezoelectric field component $F_{x'}$ can be neglected, as for the measurements under the metal stripe [Fig. 1(b)], the relevant band profiles are those of Fig. 2(a). As a consequence, recombination occurs preferentially around $\phi=3\pi/4$, where n is the largest and the e-hh transition energy the smallest, thus leading to the stronger intensity of the low-energy components of the PL doublet, as observed in Fig. 1(b).

For measurements outside the metal film, the piezoelectric potential Φ adds to the weak strain-induced band modulation. The calculated potential, together with the vertical field F_z in the QW plane, is displayed in Fig. 2(b) (the calculations neglect screening by photogenerated carrier, which can substantially weaken the potential[5]). The potential now drives the electrons toward $\phi=\pi/4$: recombination then takes place preferentially at the positions of largest band gaps, thus transferring oscillator strength to the higher-energy component of the PL doublet [cf. Fig. 1(a)]. The transfer of oscillator intensity explains the apparent blue shift of the PL line reported in previous investigations,[4,5] where no splitting was observed. The relative intensities of the splitted PL lines give thus direct information about the spatial distribution of electrons and holes in the dynamic SAW field.

Finally, the spectra in Fig. 1(a) show a small redshift of the e-hh doublets for high SAW intensities. The latter is attributed here to the quantum confined Stark effect induced by F_z. The shift, which is proportional to F_z^2, is expected from Fig. 2(b) to be the same for both doublet components.

In conclusion, we demonstrate that the strain field of a SAW spatially modulates the electronic energy level, thus leading to splitting of the PL emission energies. The relative intensities of the PL components depend on the carrier distribution in the modulated potential, which is controlled by the piezoelectric field. The investigations thus give direct insight into the dynamics of photogenerated carriers in the spatially modulated profile induced by a SAW.

We thank M. Wassermaier for comments and for a critical reading of the manuscript. Support from the Deutsche Forschungsgemeinschaft, DFG (Project Nos. SA598/2-1, GRK384, and SFB491) is also acknowledged.

*Email address: santos@pdi-berlin.de

[1] C. Weisbuch and B. Vinter, *Quantum Semiconductor Structures, Fundamentals and Applications* (Academic, San Diego, CA, 1991).

[2] S. Eshlaghi, C. Meier, D. Suter, D. Reuter, and A. D. Wieck, J. Appl. Phys. **86**, 6605 (1999).

[3] K. S. Zhuravlev, D. P. Petrov, Yu. B. Bolkhovityanov, and N. S. Rudaja, Appl. Phys. Lett. **70**, 3389 (1997).

[4] C. Rocke, S. Zimmermann, A. Wixforth, J. P. Kotthaus, G. Böhm, and G. Weimann, Phys. Rev. Lett. **78**, 4099 (1997).

[5] P. V. Santos, M. Ramsteiner, and F. Jungnickel, Appl. Phys. Lett. **72**, 2099 (1998).

[6] S. Simon, Phys. Rev. B **54**, 13 878 (1996). The numeric value of the normalization factor H in Eq. (37) is incorrect. The correct value for GaAs is $H=1.067\times10^{11}\,\mathrm{V/m^2}$.

[7] *Semiconductors Physics of Group IV Elements and III-V Compound* edited by O. Madelung, Landolt-Bornstein-New Series, Group III, Vol. 17, Pt a (Springer-Verlag, Heidelberg, 1982).

[8] G. L. Pikus and G. E. Bir, *Symmetry and Strain-Induced Effects in Semiconductors* (Wiley, New York, 1974).

[9] P. V. Santos, Appl. Phys. Lett. **74**, 4002 (1999).

[10] P. V. Santos, R. Nötzel, and K. H. Ploog, J. Appl. Phys. **85**, 8228 (1999).